Hindawi
International Transactions on Electrical Energy Systems
Volume 2022, Article ID 9474640, 13 pages
https://doi.org/10.1155/2022/9474640

Research Article

Diagnosis of Broken Bars in V/F Control Induction Motor Drive Using Wavelets and EEV Estimation for Electric Vehicle Applications

Senthil Kumar Ramu,[1] **Gerald Christopher Raj Irudayaraj**,[2] **Gunapriya Devarajan**,[3] **V. Indragandhi**,[4] **V. Subramaniyaswamy**,[5] **and J. Sam Alaric**[6]

[1]*Department of Electrical and Electronics Engineering, Sri Krishna College of Technology, Coimbatore 641042, India*
[2]*Department of Electrical and Electronics Engineering, PSNA College of Engineering and Technology, Dindigul 624622, India*
[3]*Department of Electrical and Electronics Engineering, Sri Eshwar College of Engineering, Coimbatore 641202, India*
[4]*School of Electrical Engineering, Vellore Institute of Technology, Vellore 632014, India*
[5]*School of Computing, SASTRA Deemed University, Thanjavur 613401, India*
[6]*Department of Electrical and Computer Engineering, Wollega University, Nekemte, Ethiopia*

Correspondence should be addressed to J. Sam Alaric; samalaric@gmail.com

Received 23 July 2022; Accepted 16 August 2022; Published 5 September 2022

Academic Editor: Ravi Samikannu

The induction motor (IM) defect diagnosis has been an important field of research in recent years. The development in control circuits for IM has piqued the interest of industrialists and researchers. This paper presents a method for detecting and quantifying broken rotor bar (BRB) faults via wavelets and energy Eigen value (EEV) estimation in voltage/frequency control-fed IM. The fast Fourier transform (FFT) extracts the signal's amplitude and frequency components, while the discrete wavelet transform (DWT) decomposes it. In this paper, the energy estimation for each level of breakdown and the method to overcome the diagnose faults are explained. The EEV of the motor current of the signal determines the fault's severity and provides a better method for identifying the faults. The usage of a single current sensor is a gain of this technology. With a fluctuating load, we can identify the issue and the number of broken bars via online. After processing of DWT, the faulty BRB's stator current signal is suppressed to 91% in amplitude when compared to existing techniques. Simulation and experimental results have proved that the proposed method's stability, durability, and resilience.

1. Introduction

The greatest approach would be to replace traditional internal combustion engine (ICE) automobiles with electric vehicles (EVs), which emit fewer pollution than current ICE vehicles. This is the same as reducing transportation-related air pollution to zero. The electric motor is a key component of an EV's electric powertrain (which includes the drivetrain and the motor). According to comparative research, IM is more suited for use as a traction motor in electric vehicles [1, 2]. In addition, IMs are susceptible to a variety of failures [3, 4]. The BRB defect is one of them [5]. Overloading working conditions, mechanical cracks, and manufacturing problems can all contribute to it [6]. A broken bar causes a significant rise in currents and pressures in neighboring rotor bars, potentially leading to more damage and even stator problems [3, 7]. As a result, detecting the broken bar fault at an early stage is important. The IM is designed to be a fault-tolerant computer and a more enjoyable solution for EV applications in today's reality.

BRB defects are instigated through a mixture of several loads which are imposed on the rotor by thermal, environmental, electromagnetic, mechanical, and dynamic variables. The BRBs cause speed and torque oscillations, as

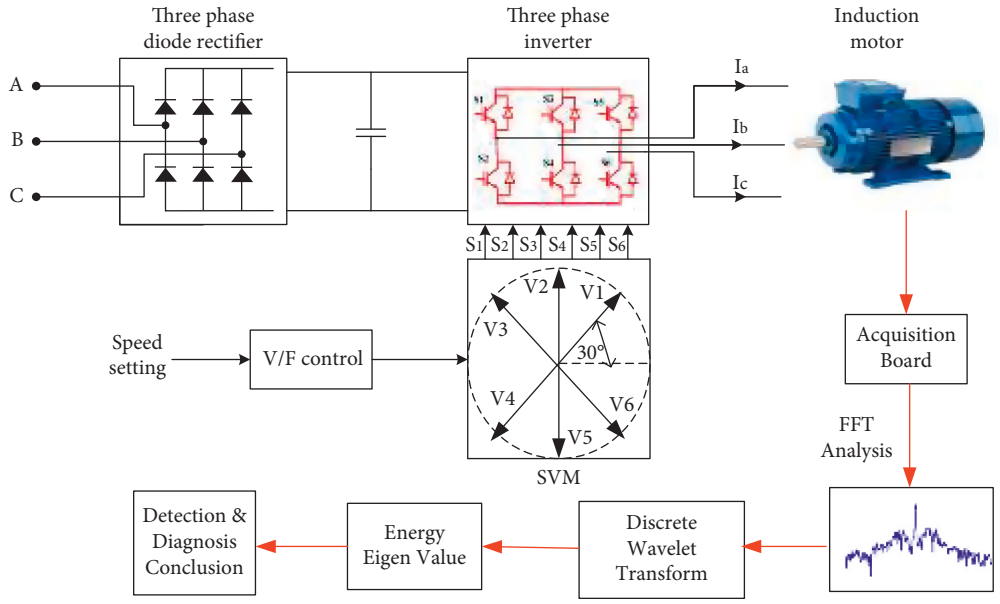

Figure 1: Block diagram of DWT and energy EEV estimation-based fault diagnosis.

well as bearing degradation that is incomplete. It can also cause rotor shaft vibrations, bearing problems, and air gap eccentricity. Also, a mixture of stress operating on the rotor causes rotor deficiency. It causes more deviations, which reduces magnitude of torque. As a result, mechanical faults and larger variations occur, which lead to disastrous consequences for the machine. BRB faults do not cause the machine to halt. It can cause extreme mechanical stress to insulation, as well as winding failure, which can result in costly repairs and production losses. With the invention of solid-state inverters, the constant V/F control became widespread [8, 9], and this type of variable speed drive is used by the huge majority of variable speed drives in use today [10]. To gain the best results, IM should function with rated stator flux. This can be accomplished by keeping the voltage constant. To gain the best results, IM should function with rated stator flux [11].

Motor current signature analysis (MCSA) is most often method for fault diagnosis of IM [12, 13]. It is indeed a noninvasive, easy, and effective approach under specific loads. As a consequence, it is in commonplace in industrial settings [14]. Instantaneous power, magnetic flux, torque, and vibrational signals are some of the other indicators used to diagnose rotor problems [15, 16]. In addition, methodologies for distinguishing between broken bar defects and moment loads have engaged a considerable number of scholars in recent years [17, 18]. The intricacy of the system that has to be diagnosed is also a factor. In the diagnostic sector, there are two types of procedures: analytical model-based diagnostic techniques and non-analytical model-based diagnostic methods [19]. The references cover a wide range of failure scenarios as well as the methods for detecting them. According to our investigation and extensive literature evaluation, signal processing is among the most important methodologies used in fault diagnosis.

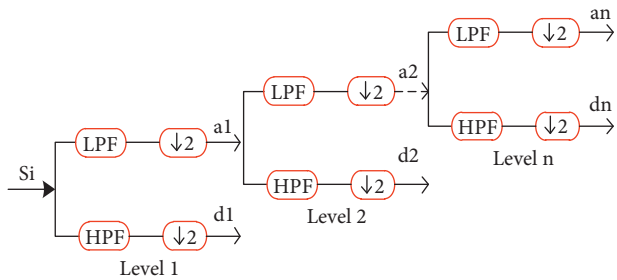

Figure 2: Decomposition using DWT.

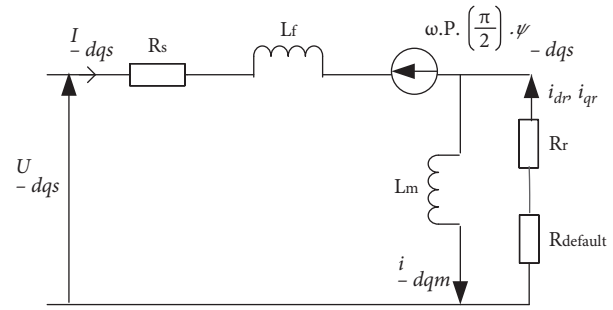

Figure 3: Equivalent circuit diagram for BRB fault IM.

The signal processing approach may be separated into two halves, the first of which uses traditional techniques such as FFT [20] and Hilbert analysis [21], and the second of which uses novel techniques such as windowed Fourier transforms and wavelet analysis [22]. Frequency examination of quantifiable variables is currently the important method utilized approach for defect analysis. One of the most significant of these approaches is the FFT. The primary drawback of this technology is that it can only be employed

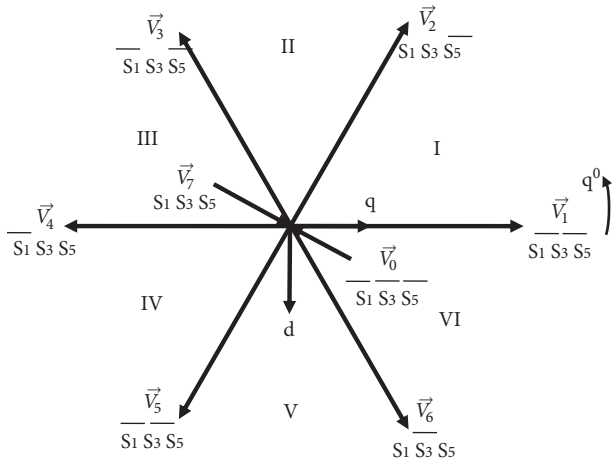

Figure 4: Space vector representation of VSI.

Table 1: Switching states and space vector representation of VSI.

Type	Switching state	On-state switch	PWM inverter voltage			Space vector
			V_{AN}	V_{BN}	V_{CN}	
Active states	[1 6 2]	S_1, S_6, S_2	V_d	0	0	$\vec{V}_1 = (2/3)V_d e^{j0}$
	[1 3 2]	S_1, S_3, S_2	V_d	V_d	0	$\vec{V}_2 = (2/3)V_d e^{j\pi/3}$
	[4 3 2]	S_4, S_3, S_2	0	V_d	0	$\vec{V}_3 = (2/3)V_d e^{j2\pi/3}$
	[4 3 5]	S_4, S_3, S_5	0	V_d	V_d	$\vec{V}_4 = (2/3)V_d e^{j3\pi/3}$
	[4 6 5]	S_4, S_6, S_5	0	0	V_d	$\vec{V}_5 = (2/3)V_d e^{j4\pi/3}$
	[1 6 5]	S_1, S_6, S_5	V_d	0	V_d	$\vec{V}_6 = (2/3)V_d e^{j5\pi/3}$
Zero states	[1 3 5]	S_1, S_3, S_5	0	0	0	$\vec{V}_7 = 0$
	[4 6 2]	S_4, S_6, S_2				$\vec{V}_0 = 0$

in a stationary state. As a result, a different approach to resolving this issue is required. Wavelet transformations can be divided into two types: continuous and discrete wavelets. Mallet et al. was the first to use multi-resolution wavelet analysis to a problem [23]. Talhaoui et al. [24] performed a similar technique for the identification of rotor problems in the IM. Other papers have utilized the DWT method to discover a number of issues, such as unbalanced eccentricity as well as stator turn short circuits [25, 26].

The importance of automated damage detection is growing for a variety of reasons, the much more notable of which being the human factor's inadequacy, as well as environmental pressures. The major goals of this work are to diagnose a BRB defect and to assess the severity of the issue while the IM is in closed loop drive with constant speed. The V/F control approach is used to attain a constant decoupled control [27, 28]. The speed regulator output signal and stator phase current will be subjected to DWT investigation as a defect identification technique. This approach was used in order to provide a good diagnosis despite the constant speed variations. The energy stored for each stage of dynamic energy may be utilized to assess the intensity of the fault and differentiate among defect and regular fluctuation.

For all frequencies and loading circumstances, DWT is appropriate for a variable size window. Low-frequency approximation signals were employed to identify BRB defects with short duration time. As a result, fast defect identification is feasible, allowing the equipment to be protected and controlled before it becomes dangerous. Figure 1 shows a block diagram of DWT and energy Eigen value-based BRB fault diagnostics.

To solve many shortcomings with earlier approaches, a solution based on EEV and wavelet packets is proposed in this paper. The key benefit of this system is that it only requires one current sensor. The proposed technique can identify a fault of broken bars with a variable load in real time, because it can determine the number of broken bars irrespective of the motor's operational mode. The most successful method for identifying abnormalities in steady-state, start, and nonstationary signals is to use this method.

In [5], Authors suggest a method for detecting BRB faults under field-oriented control using discrete wavelet coefficients. A reduced dynamic model and stator current spectrum-based fault diagnosis of IM is proposed in [29]. Fuzzy logic controller was presented for examining the performance of drive during BRB failures [30]. This technique reduces sensitivity to electrical parameter fluctuation at each reference point during variable loads. The isolation of BRB faults under low-frequency load fluctuation using Q axis voltage and current component spectrum was proposed in

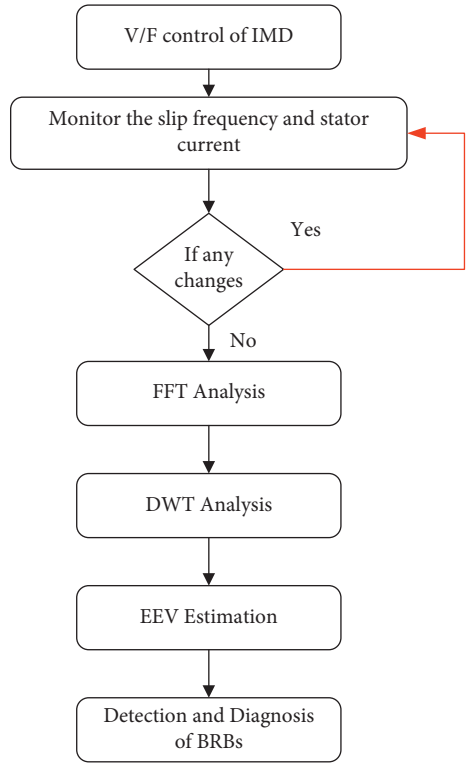

Figure 5: Fault diagnosis process.

Table 2: Induction motor parameters.

Symbol	Parameter	Values
P_0	Power output	1.1 KW
Vs	Supply voltage	440 V
Rs	Stator resistance	7.86 Ω
Rr	Rotor resistance	6.22 Ω
Lm	Mutual inductance	0.63 H
Kp	Gain constant	60
Ti	Integral constant	180
T_l	Load torque	10 Nm
n_b	Rotor bars	28

[31]. The load torque instability problem offers solutions to BRB failures with the assistance of FFTs. The main objective of this work is to diagnosis the BRB defects using DWT and EEV estimation. In this paper, both FFT and DWT are proposed for the identification of V/F-fed IMD. Then, the fault severity is calculated using EEV computation. This work aids in determining the machine's healthy and malfunctioning states and is also utilized to measure the drives' dynamic response.

The paper is organized as follows: the various signal processing techniques are discussed in Section 2. Section 3 describes the modelling of a BRB failure motor. The dynamic analysis of V/F based IMD is covered in Section 4. Section 5 looked at DWT-based BRB fault diagnosis. The findings and discussion for fault analysis are shown in Section 6, and Section 6 discusses the study's proper conclusions.

2. Signal Processing Techniques Used for Diagnosis

There are two types of defect diagnostic approaches without the use of models. The first is based on signal processing from sensors that measure various electrical and mechanical properties. Another method involves the use of different Artificial Intelligence (AI) algorithms to construct well-developed systems. In industry, signal processing and spectral analysis methods are commonly used to monitor all rotating machineries. In the current situation, employees are maintaining the stability through examining a range of signals of system in order to diagnose problems or deviations. On the other hand, the physical evolution and spectrum of such signals, give enough information for professionals to identify problems and which affects the machine's appropriate operation. The diagnosis by this method needs a proper understanding of the defect and their signs. Hence, the signal processing algorithms are favoured for diagnosing BRB defects.

2.1. FFT. The FFT algorithm is created using DFT. FFT converts a real-time signal to a frequency signal and can also be used to recover high frequency components. Therefore, the estimated magnitude and frequency can be calculated by applying the following equation after collecting a signal through FFT [32].

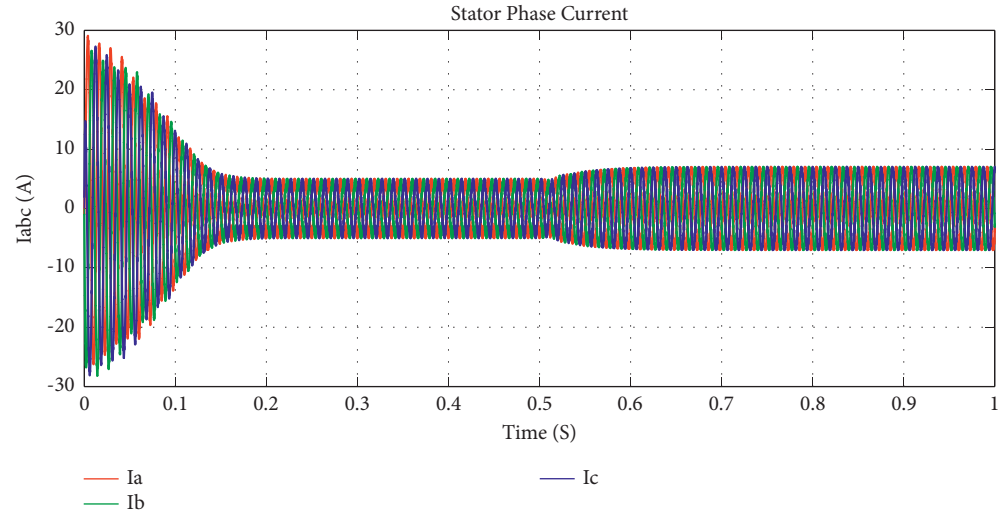

(a)

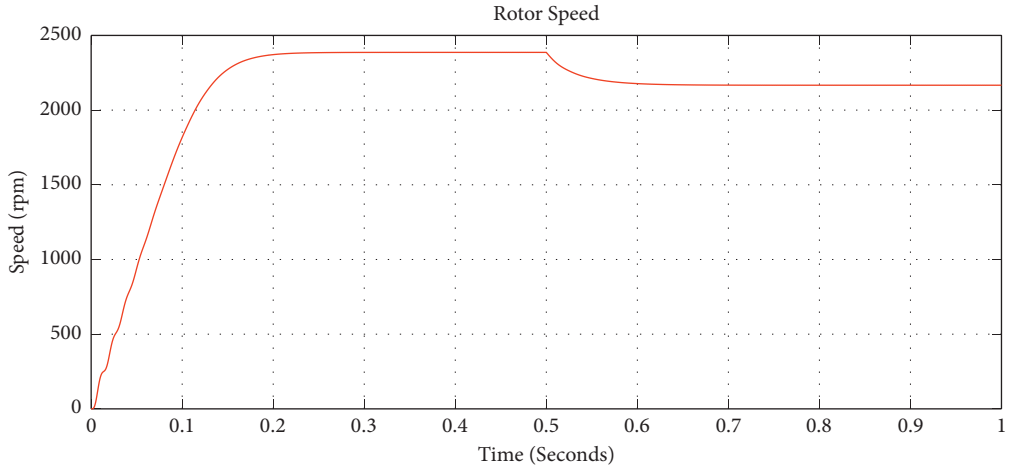

(b)

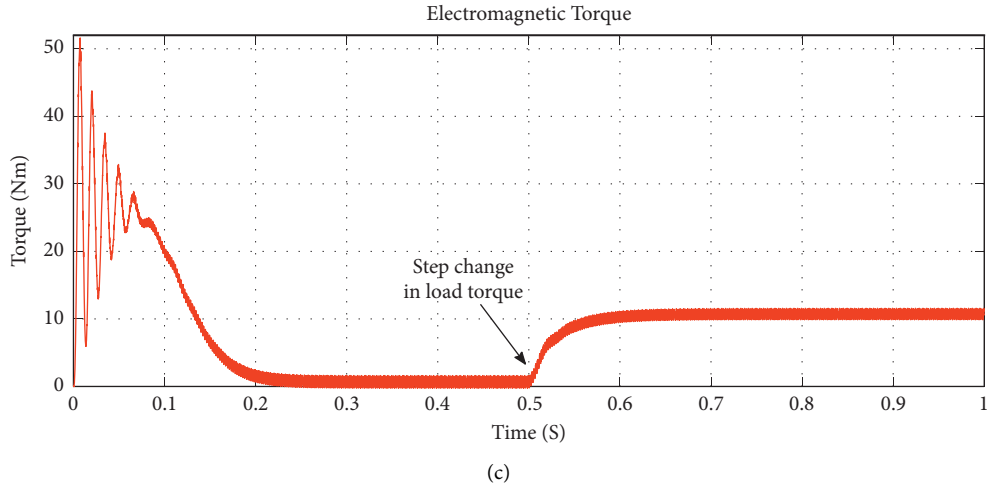

(c)

Figure 6: Simulation response of V/F control of IM at healthy state. (a) Motor current. (b) Speed. (c) Torque.

Table 3: Performance of open loop V/F control of IM under dynamic state: stator current, rotor speed when step change in load torque.

Time-domain parameters	V/F control					
	Fixed load			Full load		
	t_r (ms)	t_s (ms)	M_p (%)	t_r (ms)	t_s (ms)	M_p (%)
Stator current	73	1031	551	77	1030	541
Rotor speed	1727	1031	75	1030	1030	101.5

$$\text{Magnitude spectrum} = \frac{\sqrt{|X|^2 + |Y|^2}}{N}, \qquad \text{Phase spectrum} = \arctan\left(\frac{|Y|}{|X|}\right). \tag{1}$$

To determine the fault defect, the frequency amounts are eliminated together with amplitude. The amplitude as well as sideband frequency are altered depending on the fault under variable load conditions. The current signal from the machine is extracted and subjected to FFT analysis. Simultaneously, IM runs in a steady-state condition. The frequency components of the current signal are obtained using FFT. It is also used to determine the short circuit between the IM stator windings.

2.2. DWT. The DWT is similar to a filter bench and it is used to handle the sampling signals. Figure 2 depicts the DWT decomposition process [11].

The following formulae can be used to compute the level 1 indices:

$$a_1 = \sum_k^l L(k-2l)S_i(k), \qquad d_1 = \sum_k^l H(k-2l)S_i(k). \tag{2}$$

A next deconstruction stage is created using the a_1 indices. The updated factor can be written as follows:

$$\left\{ a_2 = \sum_k^l L(k-2l)a_1(k), d_2 = \sum_k^l H(k-2l)a_1(k). \right. \tag{3}$$

Decomposition of entire upper levels is completed. The original data is recreated and expressed as follows:

$$S' = a_n + d_n + d_{(n-1)} + \cdots + d_1. \tag{4}$$

2.3. Energy Eigen Value Estimation. Calculating EEV at every level of decomposition is an effective diagnostic technique for determining the severity of a defect. The EEV is computed using the following equation [33]:

$$E_i = \sum_{k=1}^{k=n} \left|D_{i,k}(n)\right|^2, \tag{5}$$

where i is the decomposition level. Each wavelet packet factor in a frequency range has a magnitude band of D; N is the DWT time of decomposition. The BRB diagnosis technique involves the computation of EEVs, with specific change numbers reflecting the severity of the problem.

3. Modelling of IM with BRB Faults Taken into Account

The healthy state of IM with-reference elements is modelled, and the relevant state equations are established to confirm IM performance [34]. Figure 3 relates the IM to the BRB model in terms of schematic diagram.

The rotor coordinates model of IM is represented as follows:

$$\dot{x}(t) = A(\omega)\cdot x(t) + Bu(t), \qquad y(t) = Cx(t), \tag{6}$$

where $x = \begin{bmatrix} I_{ds} & I_{qs} & \psi_{dr} & \psi_{qr} \end{bmatrix}^T$, $u = \begin{bmatrix} U_{ds} \\ U_{qs} \end{bmatrix}$, and $y = \begin{bmatrix} I_{ds} \\ I_{qs} \end{bmatrix}$.

$$A(\omega) = \begin{bmatrix} -(R_s + R_{eq})L_f^{-1} & \omega_r & R_{eq}L_m^{-1}L_f^{-1} & -\omega \\ -\omega & -(R_s + R_{eq})L_f^{-1} & -\omega L_f^{-1} & R_{eq}L_m^{-1}L_f^{-1} \\ R_{eq} & 0 & R_{eq}L_m^{-1} & 0 \\ 0 & R_{eq} & 0 & R_{eq}L_m^{-1} \end{bmatrix},$$
$$B = \begin{bmatrix} L_f^{-1} & 0 \\ 0 & L_f^{-1} \\ 0 & 0 \\ 0 & 0 \end{bmatrix},$$
$$C = \begin{bmatrix} 1 & 0 & 0 & 0 \\ 0 & 1 & 0 & 0 \end{bmatrix}. \tag{7}$$

The corresponding rotor resistance is calculated as follows:

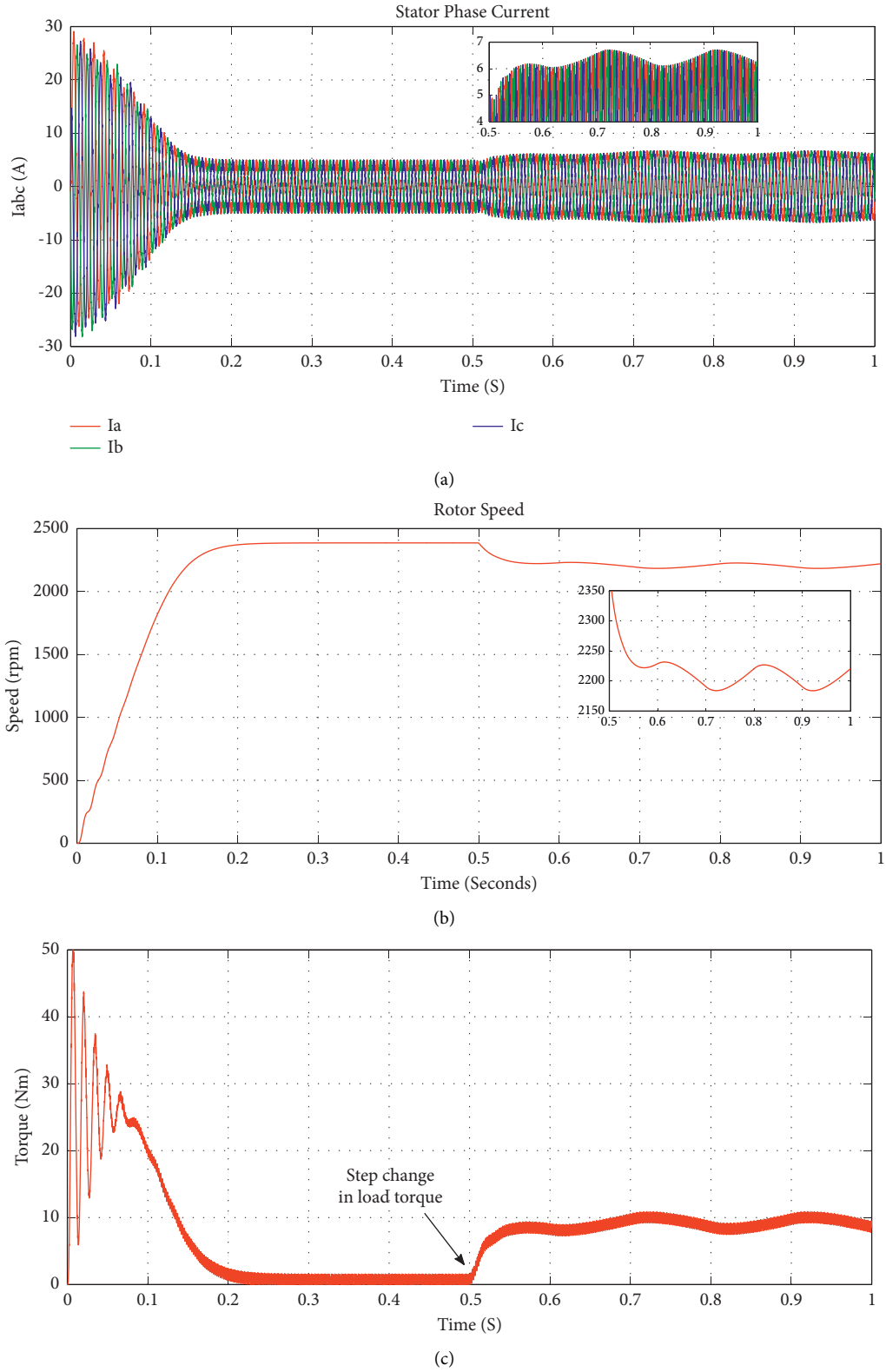

Figure 7: Simulation response of V/F control of IM at defect state. (a) Motor current. (b) Speed. (c) Torque.

Figure 8: Experimental setup.

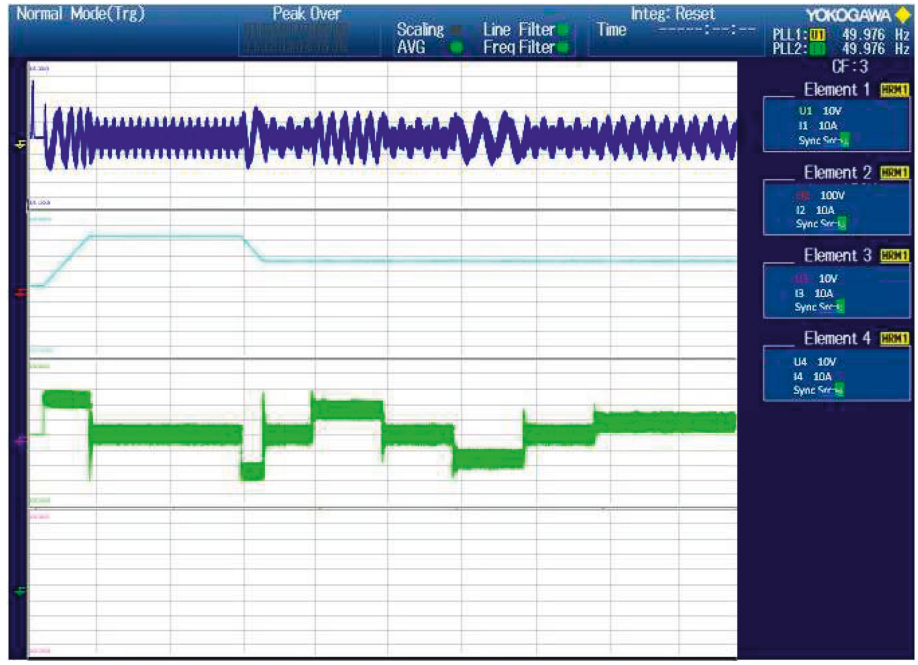

Figure 9: Experimental waveform of current, speed, and torque in V/F-fed IM under healthy state.

$$R_{eq} = R_r + \frac{\alpha}{1-\alpha} K(\theta_0) R_r,$$

$$K(\theta_0) = \begin{bmatrix} \cos(\theta_0)^2 & \cos(\theta_0)\sin(\theta_0) \\ \cos(\theta_0)\sin(\theta_0) & \sin(\theta_0)^2 \end{bmatrix}, \quad (8)$$

$$\alpha = \frac{2}{3}\zeta_0,$$

$$\zeta_0 = \frac{3n_{bc}}{n_b}.$$

4. VSI: SVM Switching

SVM is an advanced modulation system based on eight distinct switching potential combinations of VSI that is commonly achieved by digital signal processing (DSP) or microcontrollers. At the top or bottom of conduction switches, there are six active state (to) and two zero states [35].

In a *d-q* plane, the eight various states may be characterized as fixed vectors, as shown in Figure 4. The output reference vector can be generated by adding two or more vectors, with each vector's magnitude controlled by time. Table 1 depicts the different switching states and space vector representations.

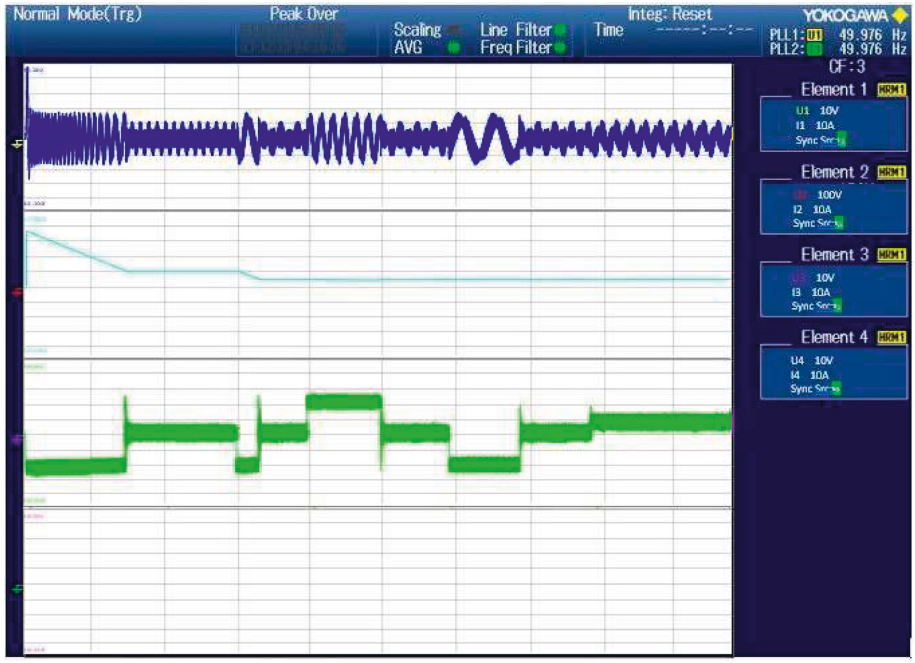

Figure 10: Experimental waveform of current, speed, and torque in V/F-fed IM under faulty state.

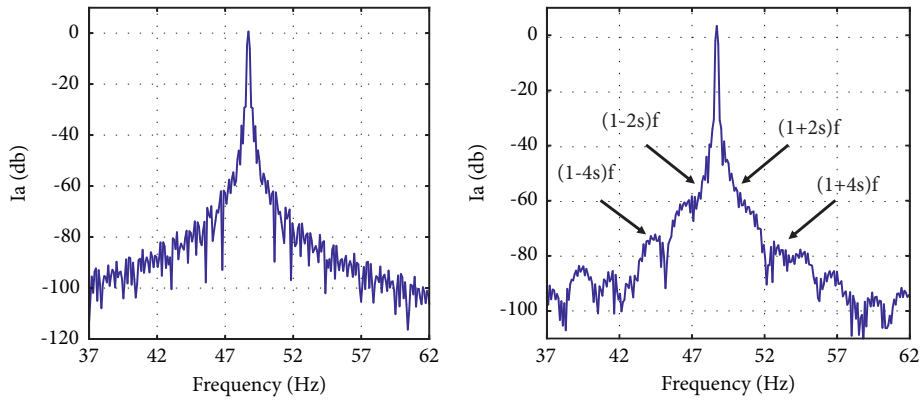

Figure 11: FFT analysis of motor current in V/F control of IM at full load condition. (a) Healthy case. (b) 2 BRBs faulty case.

Table 4: Frequency and amplitude of motor current in V/F control of IM.

Side band frequency ($s = 0.045$)	Estimated frequency (Hz)	Healthy state		Faulty state	
		Frequency (Hz)	Amplitude (dB)	Frequency (Hz)	Amplitude (dB)
(1–4 s) f_s	41	43	−82	44	−75
(1-2 s) f_s	45.5	47	−62	48	−48
(1 + 2 s) f_s	54.5	51	−61	52	−50
(1 + 4 s) f_s	59	54	−81	55	−70

5. Fault Diagnosis of IMD

The proposed fault diagnosis method is depicted in Figure 5 as a flow chart. The V/F control method is evaluated using 1.1 kW, 440 V, 28 rotor bars to verify the established BRB model. Table 2 contains the simulation and experimental parameters for IM. The MATLAB function is used to conduct the section of the diode bridge

Table 5: Frequency band of wavelet coefficients of V/F fed IM.

Levels	Frequency band
d_1	12250–25000 Hz
d_2	6125–12250 Hz
d_3	3062.5–6125 Hz
d_4	1531.25–3062.5 Hz
d_5	765.625–1531.25 Hz
d_6	382.81–765.625 Hz
d_7	191.40–382.81 Hz
d_8	95.70–191.40 Hz
d_9	47.85–95.70 Hz
d_{10}	23.926–47.85 Hz
d_{11}	11.96–23.926 Hz
d_{12}	5.98–11.96 Hz
a_{12}	2.99–5.98 Hz

rectifier. It is defined as a user-defined function. The RMS voltage, frequency, and time are estimated using the parameters integrated with the function.

5.1. Healthy State of IM. The machine may be controlled using the V/F control system and the SVM technology. IM's load torque and rotor speed are 2400 rpm and 10 Nm, respectively. Figure 6 shows the simulation results for motor current, rotor speed, and electromagnetic torque. When the machine is in good working condition, it produces a high current flow in the transient stage, which then becomes sinusoidal. In response to a step-variation in load torque, the machine's rotor speed achieves the nominal value and gradually drops. The step change in load torque from no load to full load is achieved between 0.5 seconds. A small decrease in IM happens after 0.5 seconds as a result of these load fluctuations. When the load torque varies, the performance of the motor current and rotor speed of the IM is shown in Table 3.

5.2. Faulty State of IM. A simplified state-space model of IM rotor failure is used to simulate the fault state of V/F control. The BRB faults may be seen in the stator current and rotor speed which are shown in Figure 7. After 0.5 seconds, the oscillations in stator current are detected while the machine runs at 2 BRBs failure state. The existence of the inverse field on the rotor ($-s\omega_s$ to $s\omega_s$) causes BRB failure. In stator winding, these two fields can interact with each other, and it increases the frequency components of $2s\omega_s$. This causes oscillations in electromagnetic torque, rotor speed, and stator current shape deviations.

5.3. Experimental Setup and Results. Figure 8 shows the IM experimental setup, which includes a condition monitoring system, a failure simulator, and a TMS320F2812 DSP processor. Gate pulses are sent to the DSP with the code composer studio. Several types of fault tests are performed utilizing a fault simulator to evaluate the efficiency of IM. To investigate the drive performance in a defective state, two tiny holes of 6 mm diameter must be bored in the rotor bars. The current sensor and the speed sensor send signals to the DSP processor. The sample is then sent to MATLAB for wavelet coefficients.

Figure 9 depicts the healthy state IM experiment results for current, speed, and load torque. The motor current (1 Div. = 2 A) balances respective rated current depending on the load fluctuations. The rotor speed (1 Div. = 100 rpm) response exhibits reduced peak overshoot and the torque (1 Div. = 2 Nm) approaches reference torque in fast. When there is a variation in torque, the oscilloscope records the variation. Figure 10 depicts an experiment V/F supplied driving waveform for both a normal and a defect motor. The motor current is abruptly raised which results in minor oscillations during the transient stage. The speed response is changed at the transient stage due to the influence of the BRB fault. It can be seen that the torque does not retain excellent dynamics.

5.4. FFT Analysis. Figure 11 shows an FFT investigation of motor current both in balanced and defective state. The FFT analysis in MATLAB/Simulink, and also the associated data, has been validated. Depending on the type of defect, the frequency and amplitude portion of harmonic in the motor current changes. Table 4 shows the frequency of sideband elements and amplitude under full load circumstances.

The FFT results demonstrate the potential for signal extraction to identify and localize BRB problems discovered in stator current. FFT has the drawback of potentially losing some time-domain information from the signal. It is challenging to process each frequency channel's assumption when the original signal is decomposed. In order to solve this issue, DWT is proposed for decompose the signal.

Table 5 shows the frequency level band of several wavelet coefficients. It provides a clear interpretation of the variables induced by the BRB fault, as the formation of harmonics during transients and steady-state condition. Figures 12 and 13 illustrate DWT analysis of stator current in healthy and defective states, respectively. The oscillations are the major contributing element for the emergence of transitioning process. There is no oscillation in the system when the wavelet signal intensity is high. In the defective condition, the stator current magnitude has high-level coefficients and variations in coefficients as compared to a healthy condition. The effect of frequency bands is influenced by BRBs failure which causes the coefficient to increase. After decomposing process, the stator current signal is reduced up to 91% in amplitude.

5.5. Energy Eigen Value Computation. The DWT nonstationary analysis shows the presence of faults. The deviation of energy eigenvalue of stator current in each level of DWT provides details regarding fault severity, as illustrated in Figure 14.

The growth in approximation and detail signals, particularly in the level corresponding to the frequency band, is validated through the assessment of energy stored in each

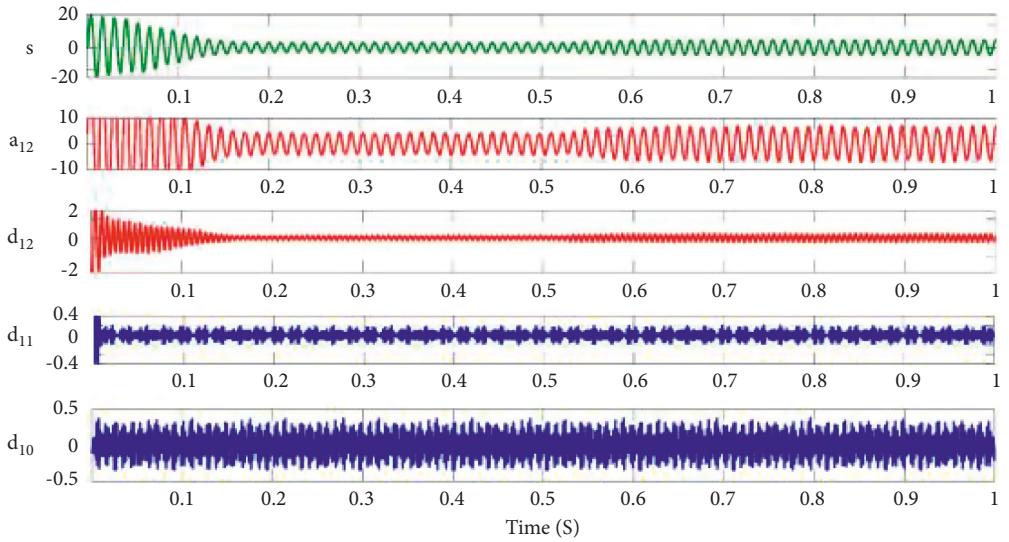

Figure 12: DWT of stator current under healthy state in V/F-fed IM.

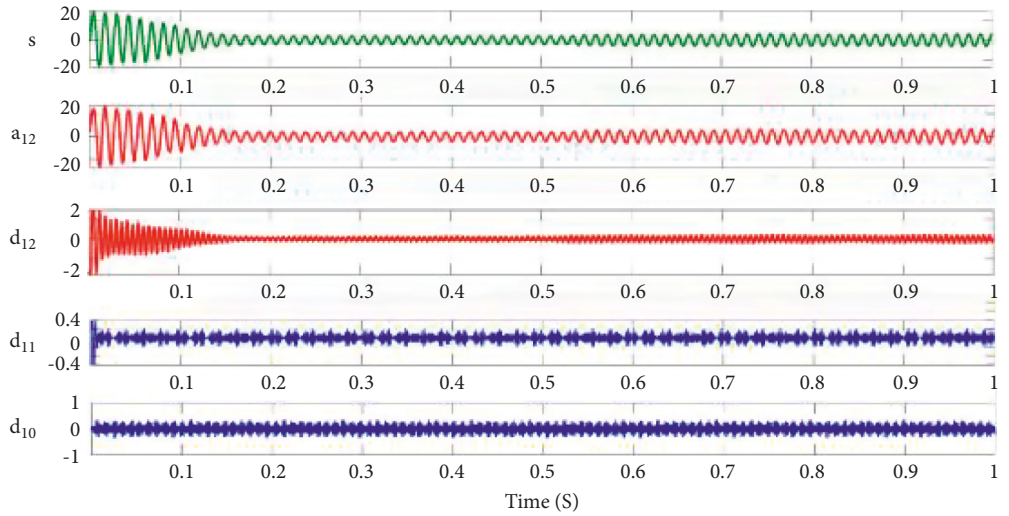

Figure 13: DWT of stator current under faulty state in V/F-fed IM.

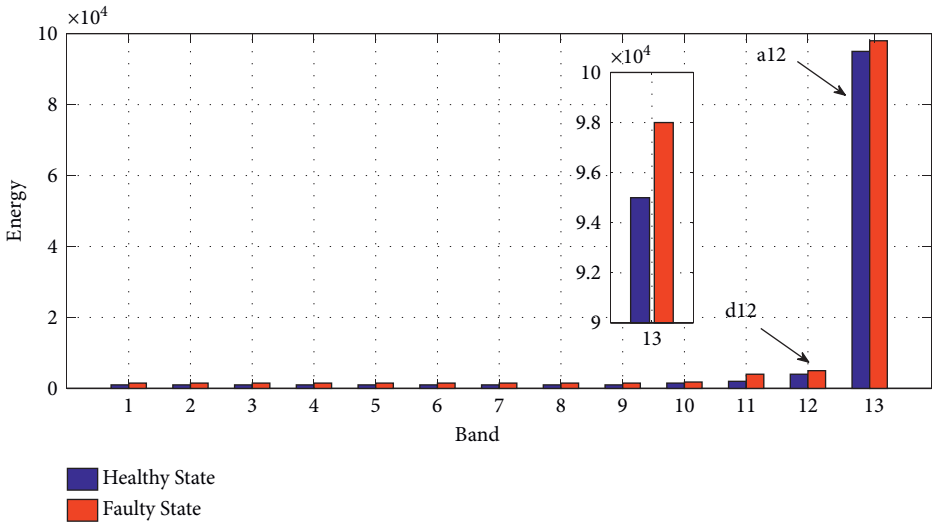

Figure 14: EEV of stator current in V/F fed IM.

decomposition level a_{12}. In level 12, the number of deviations is proportional to the EEV. The obtained result is considered as a good fault severity indicator in V/F control of IM.

6. Conclusion

Identifying and diagnosing faults with speed drives is extremely challenging. Rotor bar design is an important aspect of IMD. The machine will get affected due to the fault that occurs in the broken bars with varying loads. This paper focuses on BRB faults and the performance of the induction motor in balanced and unbalanced state. In this paper, BRB fault diagnosis in V/F control of IM is proposed. The magnitude and sideband frequencies are obtained using the FFT method. The magnitude and frequency values are obtained from the FFT outputs. To obtain the stator current and rotor speed, the DWT method is used. By calculating the EEV, we can determine the fault severity. When DWT is applied, the stator current signal of the defective BRB is suppressed to 91% of its original amplitude. The result has proved that DWT and EEV calculation are the effective methods for fault diagnosis, and it is easy to use in motor control applications. In future, the BRB fault diagnosis in vector control methods using advanced regulators will be considered. Also, introducing various observers like sliding model control and backstepping control will be utilized for BRB fault diagnosis in various control methods.

Data Availability

No data were used to support this study.

Conflicts of Interest

The authors declare that they have no conflicts of interest.

Acknowledgments

This study was conducted as a part of the Wollega University, Ethiopia.

References

[1] D. Gao, X. Lin, and Q. Yang, "Design and application of a fault diagnosis and monitoring system for electric vehicle charging equipment based on improved deep belief network," *International Journal of Control, Automation and Systems*, vol. 20, no. 5, pp. 1544–1560, 2022.

[2] S. K. Gundewar and P. V. Kane, "Condition monitoring and fault diagnosis of induction motor," *Journal of Vibration Engineering & Technologies*, vol. 9, no. 4, pp. 643–674, 2020.

[3] A. Allal and A. Khechekhouche, "Diagnosis of induction motor faults using the motor current normalized residual harmonic analysis method," *International Journal of Electrical Power & Energy Systems*, vol. 141, Article ID 108219, 2022.

[4] M. Abd-el-Malek, A. K. Abdelsalam, and O. E. Hassan, "Induction motor broken rotor bar fault location detection through envelope analysis of start-up current using Hilbert transform," *Mechanical Systems and Signal Processing*, vol. 93, pp. 332–350, 2017.

[5] T. Ameid, A. Menacer, H. Talhaoui, and Y. Azzoug, "Discrete wavelet transform and energy eigen value for rotor bars fault detection in variable speed field-oriented control of induction motor drive," *ISA Transactions*, vol. 79, pp. 217–231, 2018.

[6] A. Choudhary, D. Goyal, S. L. Shimi, and A. Akula, "Condition monitoring and fault diagnosis of induction motors: a review," *Archives of Computational Methods in Engineering*, vol. 26, no. 4, pp. 1221–1238, 2018.

[7] P. Sangeetha, "Rational-dilation wavelet transform based torque estimation from acoustic signals for fault diagnosis in a three-phase induction motor," *IEEE Transactions on Industrial Informatics*, vol. 15, no. 6, pp. 3492–3501, 2019.

[8] H. Talhaoui, T. Ameid, O. Aissa, and A. Kessal, "Wavelet packet and fuzzy logic theory for automatic fault detection in induction motor," *Soft Computing*, 2022.

[9] D. Granda, W. G. Aguilar, D. Arcos-Aviles, and D. Sotomayor, "Broken bar diagnosis for squirrel cage induction motors using frequency analysis based on MCSA and continuous wavelet transform," *Mathematical and Computational Applications*, vol. 22, no. 2, p. 30, 2017.

[10] Q. Fu, S. Yue, B. He, and N. Fu, "Multiple coupled circuit modelling approach for squirrel cage induction machine under single-broken-bar fault with stator winding functions decomposed in $d-q$ rotor reference frame," *IET Electric Power Applications*, vol. 13, no. 7, pp. 889–900, 2019.

[11] I. Harzelli, A. Menacer, and T. Ameid, "A fault monitoring approach using model-based and neural network techniques applied to input-output feedback linearization control induction motor," *Journal of Ambient Intelligence and Humanized Computing*, vol. 11, no. 6, pp. 2519–2538, 2019.

[12] O. E. Hassan, M. Amer, A. K. Abdelsalam, and B. W. Williams, "Induction motor broken rotor bar fault detection techniques based on fault signature analysis—a review," *IET Electric Power Applications*, vol. 12, no. 7, pp. 895–907, 2018.

[13] S. O. Ibrahim, K. N. Faris, and E. A. Elzahab, "Implementation of fuzzy modeling system for faults detection and diagnosis in three phase induction motor drive system," *Journal of Electrical Systems and Information Technology*, vol. 2, no. 1, pp. 27–46, 2015.

[14] O. A. Imoru, M. A. Bhaskar, A. A.-G. Jimoh, and Y. Hamam, "Diagnosis of stator shorted-turn faults in induction machines using discrete wavelet transform," *African Journal of Science, Technology, Innovation and Development*, vol. 9, no. 3, pp. 349–355, 2017.

[15] M. Jannati, A. Monadi, N. R. N. Idris, and M. J. Abdul Aziz, "Experimental evaluation of FOC of 3-phase IM under open-phase fault," *International Journal of Electronics*, vol. 104, no. 10, pp. 1675–1688, 2017.

[16] L. H. B. Liboni, R. A. Flauzino, I. N. da Silva, and E. C. Marques Costa, "Efficient feature extraction technique for diagnosing broken bars in three-phase induction machines," *Measurement*, vol. 134, pp. 825–834, 2019.

[17] W. Oñate, Y. Gallardo, R. Pérez, and G. Caiza, "Comparative analysis of high frequencies for the broken bar fault diagnosis using MCSA and park's vector demodulation," *Smart Innovation, Systems and Technologies*, pp. 119–130, Springer, Berlin, Germany, 2021.

[18] A. Verma, P. Arvind, S. Sarangi, J. Kumar, and Anumeha, "Detection of broken rotor bar fault in an induction motor employing motor current signature analysis," *Recent Advances in Power Electronics and Drives*, pp. 523–530, Springer, Berlin, Germany, 2022.

[19] S.-H. Im and B.-G. Gu, "Study of induction motor inter-turn fault part II: online model-based fault diagnosis method," *Energies*, vol. 15, no. 3, p. 977, 2022.

[20] R. Senthil Kumar, I. Gerald Christopher Raj, K. P. Suresh et al., "A method for broken bar fault diagnosis in three phase induction motor drive system using artificial neural networks," *International Journal of Ambient Energy*, pp. 1–7, 2021.

[21] A. El Idrissi, A. Derouich, and S. Mahfoud, "Fault diagnosis of the bearing outer ring of an induction motor under DTC control by using Hilbert filter," *Digital Technologies and Applications*, pp. 802–812, Springer, Berlin, Germany, 2022.

[22] M. Defdaf, F. Berrabah, A. Chebabhi, and B. D. E. Cherif, "A new transform discrete wavelet technique based on artificial neural network for induction motor broken rotor bar faults diagnosis," *International Transactions on Electrical Energy Systems*, vol. 31, no. 4, 2021.

[23] Y. Mallet, O. de Vel, and D. Coomans, "Fundamentals of wavelet transforms," *Data Handling in Science and Technology*, pp. 57–84, Elsevier, Amsterdam, Netherlands, 2000.

[24] H. Talhaoui, A. Menacer, A. Kessal, and A. Tarek, "Experimental diagnosis of broken rotor bars fault in induction machine based on Hilbert and discrete wavelet transforms," *The International Journal of Advanced Manufacturing Technology*, vol. 95, no. 1–4, pp. 1399–1408, 2017.

[25] J. Guo, Z. Si, and J. Xiang, "A compound fault diagnosis method of rolling bearing based on wavelet scattering transform and improved soft threshold denoising algorithm," *Measurement*, vol. 196, Article ID 111276, 2022.

[26] F. He and Q. Ye, "A bearing fault diagnosis method based on wavelet packet transform and convolutional neural network optimized by simulated annealing algorithm," *Sensors*, vol. 22, no. 4, p. 1410, 2022.

[27] S. Datta, A. Chandra, and S. Chowdhuri, "High performance sensor-less V/F control of surface PMSM in voltage vector plane with ZVV injection and SMO-based position estimation method," *Electrical Engineering*, vol. 104, no. 2, pp. 657–666, 2021.

[28] K. Sundararaju, R. S. Kumar, and I. G. Raj, "Modeling and simulation of neural based speed controller for direct torque control of three phase induction motor," in *Proceedings of the TENCON 2017—2017 IEEE Region 10 Conference*, Penang, Malaysia, November 2017.

[29] H. Talhaoui, T. Ameid, and A. Kessal, "Energy eigenvalues and neural network analysis for broken bars fault diagnosis in induction machine under variable load: experimental study," *Journal of Ambient Intelligence and Humanized Computing*, vol. 13, no. 5, pp. 2651–2665, 2021.

[30] B. Saad and A. Goléa, "Direct field-oriented control using fuzzy logic type-2 for induction motor with broken rotor bars," *Advances in Modelling and Analysis C*, vol. 72, no. 4, pp. 203–212, 2017.

[31] T. Goktas and M. Arkan, "Discerning broken rotor bar failure from low-frequency load torque oscillation in DTC induction motor drives," *Transactions of the Institute of Measurement and Control*, vol. 40, no. 1, pp. 279–286, 2016.

[32] R. Senthil Kumar and I. Gerald Christopher Raj, "Broken rotor bar fault detection using DWT and energy eigenvalue for DTC fed induction motor drive," *International Journal of Electronics*, vol. 108, no. 8, pp. 1401–1425, 2021.

[33] S. R. Kapoor, N. Khandelwal, and P. Pareek, "Bearing fault analysis by signal energy calculation based signal processing technique in squirrel cage induction motor," in *Proceedings of the 2014 International Conference on Signal Propagation and Computer Technology (ICSPCT 2014)*, Ajmer, India, June, 2014.

[34] B. Bessam, A. Menacer, M. Boumehraz, and H. Cherif, "Detection of broken rotor bar faults in induction motor at low load using neural network," *ISA Transactions*, vol. 64, pp. 241–246, 2016.

[35] F. Acosta-Cambranis, J. Zaragoza, L. Romeral, and N. Berbel, "Comparative analysis of SVM techniques for a five-phase VSI based on SIC devices," *Energies*, vol. 13, no. 24, p. 6581, 2020.